DOI: 10.14529/mmph210106

FIRST-PRINCIPLES STUDIES OF THE PHASE TRANSITIONS IN Fe-Si ALLOYS

A.B. Koshkin[1], M.A. Zagrebin[1,2], V.V. Sokolovskiy[1], V.D. Buchelnikov[1]
[1]Chelyabinsk State University, Chelyabinsk, Russian Federation
[2]South Ural State University, Chelyabinsk, Russian Federation
E-mail: miczag@mail.ru

In this paper, the structural and magnetic properties of $Fe_{100-x}Si_x$ alloys ($10 \le x \le 25{,}0$ at. %) were calculated. The structural phase transition temperatures for the crystal structures A2, B2, and D03 were estimated from the geometry optimization. The Curie temperatures were calculated in a molecular-field approximation using the constants of magnetic exchange interaction calculated ab initio. For all the considered concentrations, with the temperature increase, we observed the structural transitions from the ordered cubic phase to a disordered structure, with the intermediate stage of a partially disordered state. The ferromagnet–paramagnet transition was observed for all the compositions, though in various crystal phases.

Keywords: Fe-Si; phase diagram; first-principles calculations; molecular-field approximation.

1. Introduction

Fe-Si alloys are drawing the interest of both experimentalists and theoreticians due to their possible applications in spintronic, optoelectronic, and thermionic devices [1–4]. For example, Fe_3Si is a promising material for a ferromagnetic electrode in spintronic devices, which use magnetic tunnel junctions [1]. Also, Fe_3Si is a ferromagnet with a Curie point of around 800 K, and, as a thin film, it has a spin polarization of 45 % [2]. Fe_5Si_3 is a metallic ferromagnet at room temperature, so it is also a promising material for spintronics [3]. β-$FeSi_2$, a narrow gap (~0,85 eV) semiconductor, was used to create a light-emitting diode [4].

With the increasing concentration of Si in Fe-Si alloys, its spontaneous magnetization gradually decreases [5]. For small Si concentration, this decrease is proportional to Si concentration. However, the Mossbauer spectroscopy [6] found the strong dependency of Fe magnetic moments on the nearest-neighbors' atomic environment for larger Si concentrations. Moreover, Si substitution results in a considerable decrease of the magnetic anisotropy, which makes Fe-Si alloys magnetically soft materials with potential application in the electric energy industry [5, 7].

In this work, we investigated the structural and magnetic phase transitions of $Fe_{100-x}Si_x$ alloys ($10 \le x \le 25{,}0$ at.%) using *ab initio* calculations.

2. Simulation details

For investigating the structural and magnetic properties of $Fe_{100-x}Si_x$ alloys ($10 \le x \le 25{,}0$ at. %), we used SPR-KKR (a spin-polarized relativistic Korringa–Kohn–Rostoker) code [8], which is based on the Korringa-Kohn-Rostoker Greens function method. Geometry optimization was performed for experimentally observed Fe-Si structures: the ordered phase $D0_3$ (symmetry group $Fm\bar{3}m$ no. 225, BiF_3-type structure), the partially disordered phase B2 (symmetry group $Pm\bar{3}m$ no. 221, CsCl-type structure), and the disordered phase A2 (symmetry group $Im\bar{3}m$ no. 229, α-Fe-type structure). The equilibrium lattice parameters a_0 were obtained from the dependency of total energy E_0 on the cell volume with a fitting to the Birch–Murnaghan equation of states. For the exchange-correlation potential, we used the general gradient approximation in the form of Perdew–Burke–Ernzerhof functional [9]. The obtained equilibrium lattice parameters were used to calculate the exchange interaction parameters J_{ij} via SPR-KKR code. The disorder (both structural and chemical) in phases $D0_3$, B2, and A2 was created by the coherent potential approximation [8]. Magnetic exchange interaction parameters were calculated by using the spin-polarized scalar-relativistic Dirac Hamiltonian in the local density approximation (Vosko–Wilk–Nusair

functional [10]). The obtained magnetic exchange interaction parameters were used to estimate the Curie point T_C in the mean field approximation [11].

3. Results and Discussion

The geometry optimization showed that the most energetically favorable structure is $D0_3$ for all considered concentrations $Fe_{100-x}Si_x$. Table 1 presents the results of a_0 calculations for different Si concentrations, obtained via SPR-KKR code. The calculated lattice parameters were obtained for A2, B2, and $D0_3$ phases. The values calculated via VASP package, a_0^{th}, [12] and experimentally observed ones, a_0^{exp}, [13–15] are also present. SPR-KKR results are slightly larger than the VASP-calculated and experimental lattice parameters. Also, Table 1 shows that for B2 and $D0_3$ phases, the lattice parameter decreases with the increase of Si concentration since Si atomic radius (1,18 Å) is smaller than Fe one (1,26 Å). A2 phase has similar a_0 values for all the considered Si concentrations due to the disordered structure. The discrepancy between a_0^{exp} and a_0 can be explained by the different temperature regimes: the experiments were conducted at room temperature, while the calculations obtained the ground states (T = 0 K).

Table 1

The equilibrium lattice parameters a_0 (Å) for A2, B2, and $D0_3$ phases. a_0^{th} is taken from [12], a_0^{exp} – from [13–15]

x	Phase	a_0	a_0^{th}	a_0^{exp}
10	A2	2,870	–	2,86031[1]
	B2	2,865	–	–
	$D0_3$	5,727	–	–
15	A2	2,870	2,840[4]	–
	B2	2,855	2,826[4]	2,84844[2]
	$D0_3$	5,708	5,65[4]	–
20	A2	2,871	–	2,85591[1]
	B2	2,842	–	2,83748[2]
	$D0_3$	5,680	–	–
22	A2	2,874	2,833[5]	–
	B2	2,836	2,807[6]	2,83319[2]
	$D0_3$	5,671	5,63[5]	–
23	A2	2,871	–	–
	B2	2,832	–	–
	$D0_3$	5,665	–	–
24	A2	2,872	–	–
	B2	2,829	–	–
	$D0_3$	5,659	–	–
25	A2	2,872	2,814[6]	2,8551[1]
	B2	2,826	2,797[6]	2,82725[2]
	$D0_3$	5,650	5,61[6]	5,66[3]

[1][14], [2][15], [3][13], [4]x = 15,625 at. %; [5]x = 21,875 at. %; [6]x = 25 at. %

Fig. 1 shows the dependence of the difference between the structure total energy and the total energy corresponding to the most energetically favorable phase ($D0_3$) on Si concentration, calculated with the SPR-KKR code. For all considered concentrations, the transition from the ordered $D0_3$ phase to the disordered A2 phase through the partially disordered B2 phase was observed. This result is consistent with the calculations with the projector-augmented wave method and periodic boundary conditions implemented in VASP. The discrepancies between a_0 and a_0^{th} could be explained by the difference in structure formation: in this work, we used the coherent potential approach, which gives some averaged structure, while in [12] only one configuration was considered.

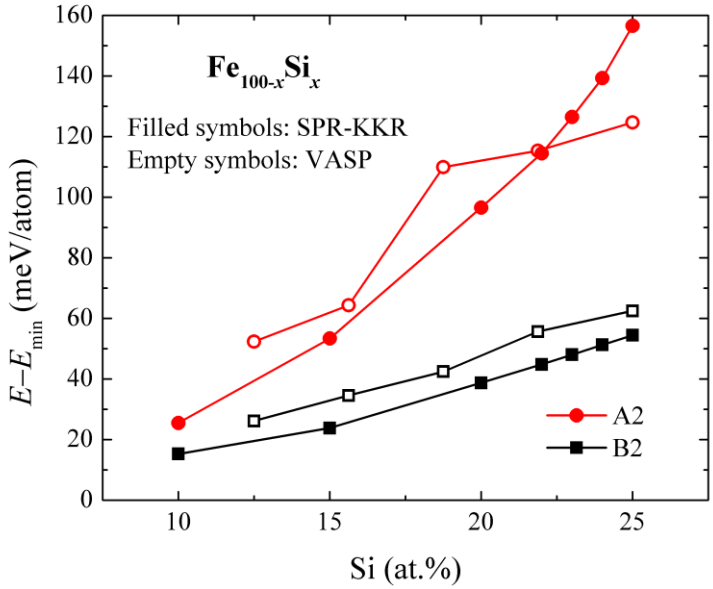

Fig. 1. Dependence of the structure total energy (in relation to the most energetically favorable phase $D0_3$) for A2 and B2 phases on Si concentration. Empty symbols present the results from [12]

By using the energy difference, we roughly estimated the temperature of a structural phase transition, T^{tr}, from the expression, $\Delta E = k_B T^{tr}$, where k_B is the Boltzmann constant, $\Delta E = E_0 - E_{min}$. We used the proportion of 1 meV = 11,60 K.

Fig. 2 presents the dependence of the total magnetic moment (per atom) on Si concentration in $Fe_{100-x}Si_x$ alloys. For all structures, the total magnetic moment per atom decreases with Si concentration increase, which could be explained by the smaller magnetic moment of Si in comparison with Fe. Fig. 2 also shows the experimental results from [13, 16], which are in quantitative agreement with the calculated values. The closest to the experiment are phases B2 and $D0_3$. Further, the obtained equilibrium lattice parameters were used to estimate the exchange interaction parameters J_{ij}, which allowed us to calculate the Curie point T_C in the molecular field approximation.

Fig. 3 shows the dependence of the Curie point T_C for phases A2, B2, and $D0_3$ of $Fe_{100-x}Si_x$ alloys on Si concentration. With the rise of Si concentration, T_C decreases for each considered phase. Similar results were obtained in the experiments [13, 17]. The qualitative agreement between the calculated and experimental T_C could also be noted.

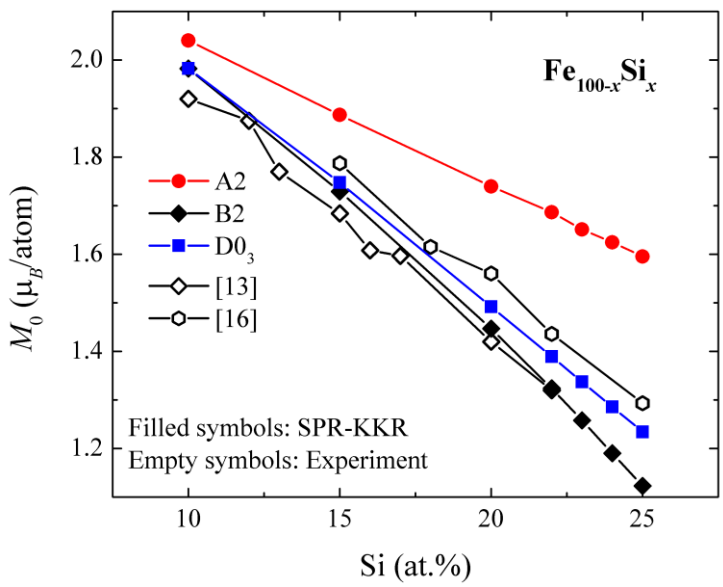

Fig. 2. Dependence of the total magnetic moment (per atom) on Si concentration in $Fe_{100-x}Si_x$ alloys. Empty symbols present the experimental results from [13, 16]

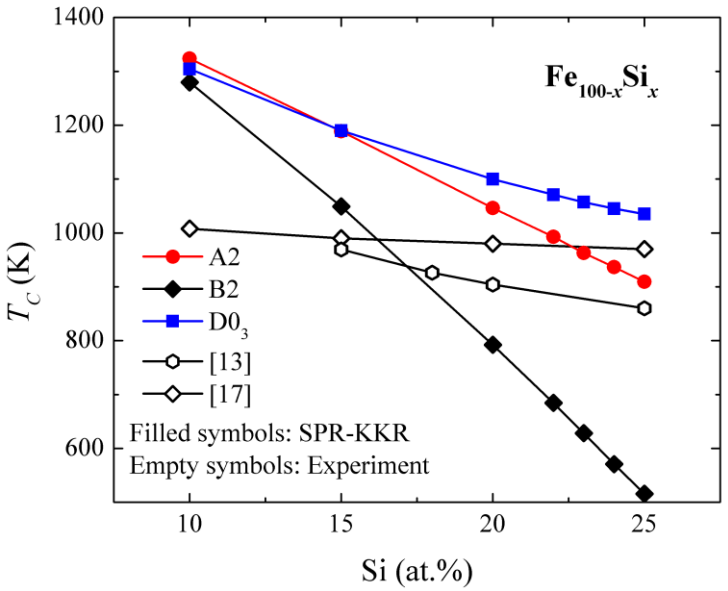

Fig. 3. Dependence of the Curie point T_C of $Fe_{100-x}Si_x$ alloys on Si concentration. Empty symbols present the experimental results from [13, 17]

Fig. 4 presents temperatures of $Fe_{100-x}Si_x$ magnetic and structural phase transitions depending on Si concentration. Dashed lines correspond to the Curie points T_C of the considered phases. A bold line with pentagons presents the temperature of a transition "paramagnet-ferromagnet" in the energetically favorable structural phase. With the temperature rise, the transition from $D0_3$ (FM) phase to B2 (FM) and then to A2 (FM) happens at Si concentrations lower than 18 at. %. The same transitions were observed experimentally for $Fe_{90}Si_{10}$ alloy [18].

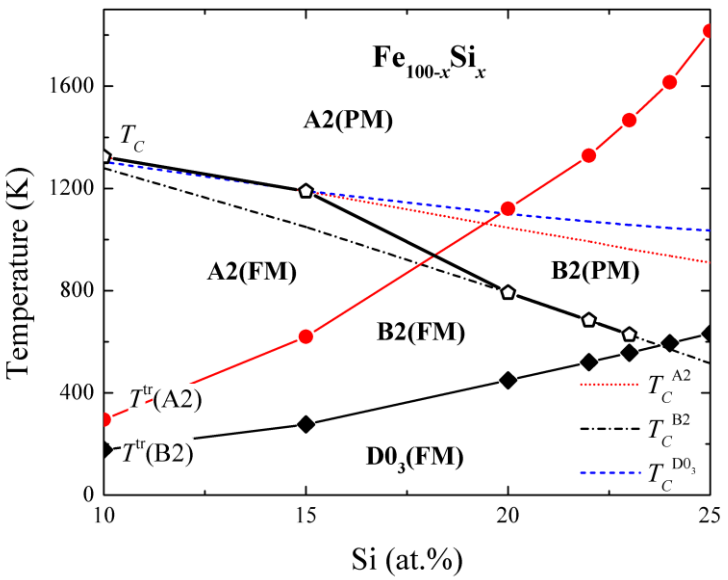

Fig. 4. *T-x* phase diagram of structural and magnetic transitions in $Fe_{100-x}Si_x$ alloys

4. Conclusions

Using *ab initio* calculations, we investigated the structural and magnetic phase transitions in $Fe_{100-x}Si_x$ ($10 \le x \le 25$ at. %) alloys. The structural phases A2, B2, and $D0_3$ were modeled. We found that all these phases are stable, and $D0_3$ is the most energetically favorable one for the considered Si concentrations.

Both the equilibrium lattice parameter and the total magnetic moment (per atom) decrease with the Si concentration increase because of the smaller atomic radius and magnetic moment of Si in comparison with Fe. The obtained results for lattice parameters and magnetic moments agree with the available experimental and theoretical data.

We estimated the temperature of structural phase transitions and showed that these temperatures decrease with the rise of Si concentration, which qualitatively agrees with the experimental data. After calculating the temperatures of the structural and magnetic transitions, we plotted the phase diagram for $Fe_{100-x}Si_x$ ($10 \le x \le 25$ at. %), which agrees with the available experimental results for Fe-Si alloys.

This work was performed with the support of the Ministry of Science and Higher Education of the Russian Federation within the framework of the Russian State Assignment under contract No. 075-00250-20-03 (sections 2 and 3). A. Koshkin gratefully acknowledges the Advanced science research foundation of the Chelyabinsk State University.

References

1. Mantovan R., Georgieva M., Fanciulli M., Goikhman A., Barantcev N., Lebedinskii Y., and Zenkevich A. Synthesis and Characterization of Fe_3Si/SiO_2 Structures for Spintronics. *Phys. Status Solidi (A)*, 2008, Vol. 205, Iss. 8, pp. 1753–1757. DOI: 10.1002/pssa.200723464.

2. Ionescu A., Vaz C.A.F., Trypiniotis T., Gürtler C.M., Garcia-Miquel H., Bland J.A.C., Vickers M.E., Dalgliesh R.M., Langridge S., Bugoslavsky Y., Miyoshi Y., Cohen L.F., Ziebeck K.R.A. Structural, Magnetic, Electronic, and Spin Transport Properties of Epitaxial Fe_3Si/GaAs(001). *Phys. Rev. B*, 2005, Vol. 71, Iss. 9, pp. 094401. DOI: 10.1103/PhysRevB.71.094401

3. Seo K., Lee S., Jo Y., Jung M.H., Kim J., Churchill D.G., Kim B. Room Temperature Ferromagnetism in Single-Crystalline Fe_5Si_3 Nanowires. *J. Phys. Chem. C.*, 2009, Vol. 113, Iss. 17, pp. 6902–6905. DOI: 10.1021/jp902010j

4. Leong D., Harry M., Reeson K.J., Homewood K.P. A Silicon/Iron-Disilicide Light-Emitting Diode Operating at a Wavelength of 1.5 μm. *Nature*, 1997, Vol. 387, pp. 686–688. DOI: 10.1038/42667

5. Wijn H.P.J. (ed.) *Soft Magnetic Alloys, Invar and Elinvar Alloys*. Berlin, Springer, Landolt–Börnstein–Group III Condensed Matter, 1994, Vol. 19, no. 1, pp. 33–143. DOI: 10.1007/b91565

6. Stearns B.M. Internal Magnetic Fields, Isomer Shifts, and Relative Abundances of the Various Fe sites in FeSi alloys. *Phys. Rev*, 1963, Vol. 129, Iss. 3, pp. 1136–1144. DOI: 10.1103/PhysRev.129.1136

7. Shin J.S., Bae J.S., Kim H.J., Lee H.M., Lee T.D., Lavernia E. J., Lee Z.H. Ordering–Disordering Phenomena and Micro-Hardness Characteristics of B2 Phase in Fe–(5–6.5%)Si Alloys. *Mater. Sci. Eng. A.*, 2005, Vol. 407, Iss. 1-2, pp. 282–290. DOI: 10.1016/j.msea.2005.07.012

8. Ebert H., Ködderitzsch D., Minár J. Calculating Condensed Matter Properties Using the KKR-Green's Function Method-recent Developments and Applications. *Reports on Progress in Physics*, 2011, Vol. 74, no. 9, pp. 096501. DOI: 10.1088/0034-4885/74/9/096501

9. Perdew J.P., Burke K., Ernzerhof M. Generalized Gradient Approximation Made Simple. *Phys. Rev. Lett.*, 1996, Vol. 77, Iss. 18, pp. 3865–3868. DOI: 10.1103/PhysRevLett.77.3865

10. Vosko S.H., Wilk L., Nusair M. Accurate Spin-Dependent Electron Liquid Correlation Energies for Local Spin Density Calculations: a Critical Analysis. *Canad. J. Phys.*, 1980, Vol. 58, no. 8, pp. 1200–1211. DOI: 10.1139/p80-159

11. Anderson P.W. Theory of Magnetic Exchange Interactions: Exchange in Insulators and Semiconductors. *Solid State Phys.*, 1963, Vol. 14, pp. 99–214. DOI: 10.1016/S0081-1947(08)60260-X

12. Zagrebin M.A., Matyunina M.V., Koshkin A.B., Buchel'nikov V.D., Sokolovskii V.V. Ab initio Studies of Phase Transformations in $Fe_{100-x}Si_x$. *Physics of the Solid State*, 2020, Vol. 62, no. 5, pp. 739–743. DOI: 10.1134/S1063783420050327

13. Varga L.K., Mazaleyrat F., Kovac J., Greneche J. M. Structural and Magnetic Properties of Metastable $Fe_{1-x}Si_x$ ($0.15<x<0.34$) Alloys Prepared by a Rapid-Quenching Technique. *Journal of Physics: Condensed Matter*, 2002, Vol. 14, no. 8, pp. 1985–2000. DOI: 10.1088/0953-8984/14/8/326

14. Miraghaei S., Abachi P., Madaah-Hosseini H.R., Bahrami A. Characterization of Mechanically Alloyed $Fe_{100-x}Si_x$ and $Fe_{83.5}Si_{13.5}Nb_3$ Nanocrystalline Powders. *J. Mater. Proc. Tech.*, 2008, Vol. 203, Iss. 1-3, pp. 554–560. DOI: 10.1016/j.jmatprotec.2007.11.064

15. Farquhar M.C.M., Lipson H., Weill A.R. An X-ray Study of Iron-Rich Iron-Silicon Alloys. *Journal of the Iron and Steel Institute*, 1945, Vol. 152, pp. 457–472.

16. Fallot M. Ferromagnetisme des Alliages de Fer. *Ann. Phys*, 1936, Vol. 11, no. 6, pp. 305–387. DOI: 10.1051/anphys/193611060305

17. Shyni P.C., Perumal A. Structural and Magnetic Properties of $Fe_{100-x}Si_x$ ($0 \le x \le 40$) Nanocrystalline Alloy Powders. *IEEE Transactions on Magnetics*, 2014, Vol. 50, no. 1, pp. 1-4, Art no. 2101904. DOI: 10.1109/TMAG.2013.2278555

18. Kubaschewski O. *Iron-binary Phase Diagrams*. Berlin, Springer, 1982, 185 p. DOI: 10.1007/978-3-662-08024-5

Received January 21, 2021

Bulletin of the South Ural State University
Series "Mathematics. Mechanics. Physics"
2021, vol. 13, no. 1, pp. 52–58

УДК 537.9 **DOI: 10.14529/mmph210106**

ПЕРВОПРИНЦИПНЫЕ ИССЛЕДОВАНИЯ ФАЗОВЫХ ПРЕВРАЩЕНИЙ В СПЛАВАХ Fe-Si

А.Б. Кошкин[1], М.А. Загребин[1,2], В.В. Соколовский[1], В.Д. Бучельников[1],
[1]Челябинский государственный университет, г. Челябинск, Российская Федерация
[2]Южно-Уральский государственный университет, г. Челябинск, Российская Федерация
E-mail: miczag@mail.ru

В работе представлены результаты расчетов структурных и магнитных свойств сплавов $Fe_{100-x}Si_x$ ($10 \le x \le 25{,}0$ ат. %). Из геометрической оптимизации для кристаллических структур A2, B2 и $D0_3$ оценены температуры структурных фазовых переходов. Температуры Кюри оценивались в приближении молекулярного поля с использованием параметров магнитного обменного взаимодействия, рассчитанных *ab initio*. Во всем рассматриваемом интервале концентраций с ростом температуры происходят структурные переходы из упорядоченной кубической фазы в частично упорядоченную, а после и в полностью разупорядоченную. Переход ферромагнетик–парамагнетик наблюдается для всех составов, однако в разных кристаллических фазах.

Ключевые слова: Fe-Si; фазовая диаграмма; первопринципные вычисления; приближение молекулярного поля.

Литература

1. Synthesis and Characterization of Fe_3Si/SiO_2 Structures for Spintronics / R. Mantovan, M. Georgieva, M. Fanciulli, A. Goikhman *et al.* // Phys. Stat. Sol. (A). – 2008. – Vol. 205, Iss. 8. – P. 1753–1757.

2. Structural, Magnetic, Electronic, and Spin Transport Properties of Epitaxial Fe_3Si/GaAs(001) / A. Ionescu, C.A.F. Vaz, T. Trypiniotis *et al.* // Phys. Rev. B. – 2005. – Vol. 71, Iss. 9. – P. 094401.

3. Room Temperature Ferromagnetism in Single-Crystalline Fe_5Si_3 Nanowires / K. Seo, S. Lee, Y. Jo *et al.* // J. Phys. Chem. C. – 2009. – Vol. 113, Iss. 17. – P. 6902–6905.

4. A Silicon/Iron-Disilicide Light-Emitting Diode Operating at a Wavelength of 1.5 μm / D. Leong, M. Harry, K.J. Reeson, K.P. Homewood // Nature. – 1997. – Vol. 387. – P. 686–688.

5. Wijn, H.P.J. (ed.) Soft Magnetic Alloys, Invar and Elinvar Alloys / H.P.J. Wijn (ed.). – Berlin, Springer, Landolt–Börnstein – Group III Condensed Matter, 1994. – Vol. 19, no. 1. – P. 33–143.

6. Stearns, B.M. Internal Magnetic Fields, Isomer Shifts, and Relative Abundances of the Various Fe Sites in FeSi Alloys / B.M. Stearns // Phys. Rev. – 1963. – Vol. 129, Iss. 3. – P. 1136–1144.

7. Ordering–Disordering Phenomena and Micro-Hardness Characteristics of B2 Phase in Fe–(5–6.5%)Si alloys / J.S. Shin, J.S. Bae *et al.* // Mater. Sci. Eng. A. – 2005. – Vol. 407, Iss. 1-2. – P. 282–290.

8. Ebert, H. Calculating Condensed Matter Properties using the KKR-Green's Function Method – Recent Developments and Applications / H. Ebert, D. Ködderitzsch, J. Minár // Reports on Progress in Physics. – 2011. – Vol. 74, no. 9. – P. 096501.

9. Perdew, J.P. Generalized Gradient Approximation Made Simple / J.P. Perdew, K. Burke, M. Ernzerhof // Phys. Rev. Lett. – 1996. – Vol. 77, Iss. 18. – P. 3865–3868.

10. Vosko, S.H. Accurate Spin-Dependent Electron Liquid Correlation Energies for Local Spin Density Calculations: a Critical Analysis / S.H. Vosko, L. Wilk, M. Nusair // Canad. J. Phys. – 1980. – Vol. 58, no. 8. – P. 1200–1211.

11. Anderson, P.W. Theory of Magnetic Exchange Interactions: Exchange in Insulators and Semiconductors / P.W. Anderson // Solid State Phys. – 1963. – Vol. 14. – P. 99–214.

12. Ab initio Studies of Phase Transformations in $Fe_{100-x}Si_x$ / M.A. Zagrebin, M.V. Matyunina, A.B. Koshkin *et al.* // Physics of the Solid State. – 2020. – Vol. 62, no. 5. – P. 739–743.

13. Structural and Magnetic Properties of Metastable $Fe_{1-x}Si_x$ ($0.15<x<0.34$) alloys prepared by a rapid-quenching technique / L.K. Varga, F. Mazaleyrat, J. Kovac, J.M. Greneche // Journal of Physics: Condensed Matter. – 2002. – Vol. 14, no. 8. – P. 1985–2000.

14. Characterization of Mechanically Alloyed $Fe_{100-x}Si_x$ and $Fe_{83.5}Si_{13.5}Nb_3$ Nanocrystalline Powders / S. Miraghaei, P. Abachi, H.R. Madaah-Hosseini, A. Bahrami // J. Mater. Proc. Tech. – 2008. – Vol. 203, Iss. 1-3. – P. 554–560.

15. Farquhar, M.C.M. An X-ray study of iron-rich iron-silicon alloys / M.C.M. Farquhar, H. Lipson, A.R. Weill // Journal of the Iron and Steel Institute. – 1945. – Vol. 152. – P. 457–472.

16. Fallot, M. Ferromagnetisme des Alliages de Fer / M. Fallot // Ann. Phys. –1936. – Vol. 11, no. 6. – P. 305–387.

17. Shyni, P.C. Structural and Magnetic Properties of $Fe_{100-x}Si_x$ ($0 \leq x \leq 40$) Nanocrystalline Alloy powders / P.C. Shyni, A. Perumal // IEEE Transactions on Magnetics. – 2014. – Vol. 50, no. 1. – pp. 1–4, Art no. 2101904.

18. Kubaschewski, O. Iron-Binary Phase Diagrams / O. Kubaschewski. – Berlin, Springer, 1982. – 185 p.

Поступила в редакцию 21 января 2021 г.